

Longitudinal and Transverse structure functions in high Reynolds-number turbulence

Rainer Grauer¹, Holger Homann^{1,2}, Jean-François Pinton³

¹ Theoretische Physik I, Ruhr-Universität Bochum, Universitätsstr. 150, D44780 Bochum (Germany)

² Université de Nice-Sophia Antipolis, CNRS, Observatoire de la Côte d'Azur, Laboratoire Cassiopée, Bd. de l'Observatoire, 06300 Nice, France

³ Laboratoire de Physique, UMR5672, CNRS & École Normale Supérieure de Lyon, 46 allée d'Italie, F69007 Lyon (France)

Abstract. Using exact relations between velocity structure functions [1, 2, 3] and neglecting pressure contributions in a first approximation, we obtain a closed system and derive simple order-dependent rescaling relationships between longitudinal and transverse structure functions. By means of numerical data with turbulent Reynolds numbers ranging from $\Re_\lambda = 320$ to $\Re_\lambda = 730$, we establish a clear correspondence between their respective scaling range, while confirming that their scaling exponents do differ. This difference does not seem to depend on Reynolds number. Making use of the Mellin transform, we further map longitudinal to (rescaled) transverse probability density functions.

1. Introduction

Intermittency is an ubiquitous feature of fluid turbulence: the scaling properties of flow quantities differ from Kolmogorov's mean field theory [4]. For instance, in the inertial range of scales where flow properties are assumed to be independent of the details of energy injection and dissipation, the velocity increments do not have a monofractal structure. In homogeneous isotropic turbulence (HIT), two directions only matter in the computation of a velocity increment: the *longitudinal* one, $\Delta_r u$ taken along the separation and the *transverse* one, $\Delta_r v$ in which the difference of velocities components perpendicular to the separation are computed. Velocity structure functions are then defined as the ensemble average: $S_{n,m}(r) = \langle (\Delta_r u)^n (\Delta_r v)^m \rangle$. For HIT, the von Kármán-Howarth relationship taken in the inertia range, leads to Kolmogorov's 4/5th law: $(\Delta u_r)^3 = -\frac{4}{5} \langle \epsilon \rangle r$, where $\langle \epsilon \rangle$ is the mean energy dissipation rate per unit mass. While a monofractal inertial range behavior would then lead to $S_{n,0} \propto r^{\zeta_n}$ with $\zeta_n \sim n/3$, intermittency means that ζ_n is a non-linear (concave) function of n . Numerous works have been devoted to the study of the functional form of ζ_n . We focus on the possible link between the longitudinal and transverse structure functions $S_{n,0}(r)$ and $S_{0,n}(r)$. There exist theoretical arguments that longitudinal and transverse show the same scaling [5]. However, both experimental data [6, 7, 8, 9] and numerical simulations [10, 11, 12, 13] show consistently different scaling exponents for longitudinal and transverse structure functions. Whether this difference can be attributed to a persistent small scale anisotropy [14, 15] or to a finite Reynolds number effect [1] is an unsolved question to which we will come back below. Here, we note that in the case of the direct cascade in electron-magnetohydrodynamic [16] it was demonstrated numerically that the difference vanishes with increasing numerical resolution and thus is a finite Reynolds number effect.

In this article, we rather focus on the correspondence between scaling ranges of the longitudinal and transverse structure functions. Our approach is based on the observation that even though the (real space) velocity field of a turbulent flow coarse-grained at a scale r is not smooth, the structure functions are smooth (differentiable) functions of r . We thus use the structure of the Navier-Stokes equation together with assumptions to derive constitutive relationships between $S_{n,0}(r)$ and $S_{0,n}(r)$. Specifically, we shall neglect the contributions from the pressure term. We start with exact scaling expressions derived by Hill [1], Hill and Boratav [2] and Yakhot [3]; we then obtain rescaling relationships between longitudinal and transverse structure functions. Our first finding is that, after rescaling, the longitudinal and transverse structure functions share the *same* inertial range, i.e. the same width in the extent of of scales where self-similarity is observed. This is important because the question of the location and span of the inertial range is often an issue in the analysis of turbulent data at (necessarily) finite Reynolds number. We stress, however, that the value of the longitudinal and transverse scaling exponents do differ. A second outcome of our simple ansatz is a direct mapping, using the Mellin transform, of the transverse and

longitudinal probability density functions (PDFs). Differences which persist after the mapping are then due to the effect of the neglected terms, as pointed in some previous attempts by Yakhot [3] and Gotoh and Nakano [17].

2. Rescaling relations between longitudinal and transverse structure functions

Our calculation trace back to the observation by Siefert and Peinke [18] that the Kármán equation (see Kármán and Howarth [19]) relating second order longitudinal and transverse structure functions can be interpreted as a Taylor expansion of a smooth function. To see this, we start with the Kármán equation

$$S_{0,2}(r) = S_{2,0}(r) + \frac{r}{2} \frac{\partial}{\partial r} S_{2,0}(r) , \quad (1)$$

which is exact, and contains no contribution from the pressure – it is a statement of incompressibility. Siefert and Peinke [18] observed that the structure function is a smooth function of r and that if the scale r is chosen in the inertial range *i.e.* “small” compared to the integral scale L , eqn. (1) can be seen as a Taylor expansion:

$$S_{0,2}(r) \approx S_{2,0}\left(r + \frac{r}{2}\right) = S_{2,0}\left(\frac{3}{2}r\right) , \quad (2)$$

where the function $S_{2,0}$ is expanded about r for consistency with the exact relationship (1). In [18] evidence from experimental data Taylor-based Reynolds numbers between 180 and 550 was presented to support this view. The success of the approach introduced by Siefert and Peinke [18] motivated us to extend their reinterpretation of differential relations to structure functions of higher orders, making use of the exact relationships derived by Hill & Boratav [2], Hill [1] and Yakhot [3]. Hill derived these relations directly by inventing a clever matrix algorithm which allowed him to efficiently simplify the derivation and calculations. Yakhot [3], on the other hand, derived an equation for the characteristic function $Z = \langle \lambda \cdot \Delta \mathbf{u}_r \rangle$ where $\Delta \mathbf{u}_r$ denotes a velocity increment over the distance r . Structure function relations can then be obtained by differentiating the characteristic function Z .

As an illustrative example, consider the relation for even order mixed structure functions derived by Yakhot [3]:

$$\frac{\partial S_{2n,0}}{\partial r} + \frac{2}{r} S_{2n,0} + \frac{2(2n-1)}{r} S_{2n-2,2} = C_p + C_f . \quad (3)$$

The term C_p contains contributions from the (unknown) pressure field and is the reason why the system cannot be closed. The term C_f contains contributions from the large scale forcing and can safely be ignored in the inertial range as proposed by Kurien and Sreenivasan [20]. These authors also analyzed and compared these relations to measurements in atmospheric turbulence at a Taylor-based Reynolds-number of about 10 700. One of their findings was that for even order structure functions the pressure contributions can be an order of magnitude smaller than the terms directly related to the structure functions. A detailed numerical study on the role of the pressure term

has been realized by Gotoh and Nakano [17]. In order to obtain closed expressions, we shall hereafter neglect the pressure contributions. Although this assumption is quite crude, we are already able to capture the dominant features of the relationship between longitudinal and transverse structure functions, such as amplitudes and common inertial range. Pressure (or energy injection) contributions will then appear as departures from predictions of this closed system of equations.

In order to demonstrate the procedure, we start with formulas for the 4-th order structure functions and neglect contributions from the pressure and the large scale forcing (see also eqn.(11) and (13) in [20])

$$3S_{2,2}(r) \approx S_{4,0}(r) + \frac{r}{2} \frac{\partial}{\partial r} S_{4,0}(r) \approx S_{4,0}\left(\frac{3}{2}r\right), \quad (4)$$

$$\frac{1}{3}S_{0,4}(r) \approx S_{2,2}(r) + \frac{r}{4} \frac{\partial}{\partial r} S_{2,2}(r) \approx S_{2,2}\left(\frac{5}{4}r\right), \quad (5)$$

which can be combined into

$$S_{4,0}\left(\frac{3}{2}\frac{5}{4}r\right) \approx S_{0,4}(r). \quad (6)$$

For the 6th order structure functions we get similarly (see eqn.(12), (15) and (14) in [20])

$$5S_{4,2}(r) \approx S_{6,0}(r) + \frac{r}{2} \frac{\partial}{\partial r} S_{6,0}(r) \approx S_{6,0}\left(\frac{3}{2}r\right),$$

$$S_{2,4}(r) \approx S_{4,2}(r) + \frac{r}{4} \frac{\partial}{\partial r} S_{4,2}(r) \approx S_{4,2}\left(\frac{5}{4}r\right),$$

$$\frac{1}{5}S_{0,6}(r) \approx S_{2,4}(r) + \frac{r}{6} \frac{\partial}{\partial r} S_{2,4}(r) \approx S_{2,4}\left(\frac{7}{6}r\right).$$

Again, combining these equations results in the simple relation

$$S_{6,0}\left(\frac{3}{2}\frac{5}{4}\frac{7}{6}r\right) \approx S_{0,6}(r). \quad (7)$$

In general, the rescaling for even order structure functions reads

$$S_{n,0}\left(\frac{3}{2}\frac{5}{4}\dots\frac{n+1}{n}r\right) = S_{n,0}\left(\frac{\Gamma(n+2)}{2^n\Gamma^2(n/2+1)}r\right) \approx S_{0,n}(r) \quad (8)$$

In order to demonstrate that the Taylor expansion is valid also for higher order structure functions, we look at the differential relation for the 4th order structure function obtained from eqn. (4) and (5)

$$S_{04}(r) = S_{40}(r) + \frac{7}{8} \frac{dS_{40}(r)}{dr} r + \frac{1}{8} \frac{d^2S_{40}(r)}{dr^2} r^2. \quad (9)$$

In Fig. 1 we compare the longitudinal (black), transverse (blue), rescaled longitudinal (red) and the one using the differential relation (green). The difference between the rescaled longitudinal and the one using the differential relation is negligible.

In order to test our results, we use numerical data from pseudo-spectral simulations of incompressible Navier-Stokes turbulence, as described in [21] – the LATU code. A statistically stationary flow is maintained by keeping constant the Fourier modes in the two lowest shells. All results are averaged over several large-eddy turn-over times (over

\Re_λ	u_{rms}	ϵ_k	ν	dx	η	τ_η	L	T_L	N^3
730	0.192	$3.8 \cdot 10^{-3}$	$1 \cdot 10^{-5}$	$1.53 \cdot 10^{-3}$	$7.2 \cdot 10^{-4}$	0.05	1.85	9.6	4096^3
460	0.189	$3.6 \cdot 10^{-3}$	$2.5 \cdot 10^{-5}$	$3.07 \cdot 10^{-3}$	$1.45 \cdot 10^{-3}$	0.083	1.85	9.9	2048^3
320	0.187	$3.5 \cdot 10^{-3}$	$0.5 \cdot 10^{-4}$	$6.14 \cdot 10^{-3}$	$2.45 \cdot 10^{-3}$	0.12	1.85	10	1024^3

Table 1. Parameters of the numerical simulations. $\Re_\lambda = \sqrt{15u_{\text{rms}}L/\nu}$: Taylor-Reynolds number, u_{rms} : root-mean-square velocity, ϵ_k : mean kinetic energy dissipation rate, ν : kinematic viscosity, dx : grid-spacing, $\eta = (\nu^3/\epsilon_k)^{1/4}$: Kolmogorov dissipation length scale, $\tau_\eta = (\nu/\epsilon_k)^{1/2}$: Kolmogorov time scale, $L = (2/3E)^{3/2}/\epsilon_k$: integral scale, $T_L = L/u_{\text{rms}}$: large-eddy turnover time, N^3 : number of collocation points.

two in the case of $\Re_\lambda = 730$). Parameters of these high-Reynolds number simulations are given in Table 1.

Fig. 2 shows the application of the rescaling formula (8) to the 2nd, 4th, 6th and 10th order structure functions obtained from a Navier-Stokes simulation with 2048^3 grid points and parameters as described in Table (1). We choose this data set because it contains ten large-eddy turn-over times and thus provides reliable statistics for high-order structure functions. In each sub-figure of Fig. 2, the unscaled structure functions are shown in the lower part (solid lines) and the structure functions rescaled according to eqn.(8) are show on top (dashed lines). Note that the original structure functions are shifted for clarity. The effect of the rescaling-transformation (8) is two-fold: first, the amplitudes from the dissipative scales up to the integral scales are now very similar.

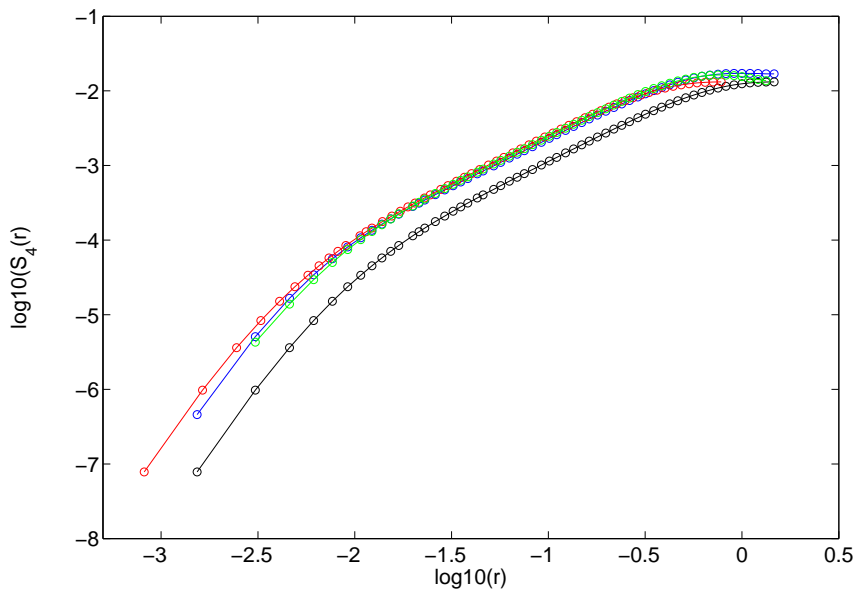


Figure 1. Comparison of structure functions: longitudinal (black), transverse (blue), rescaled longitudinal (red) and the one using the differential relation (9) (green).

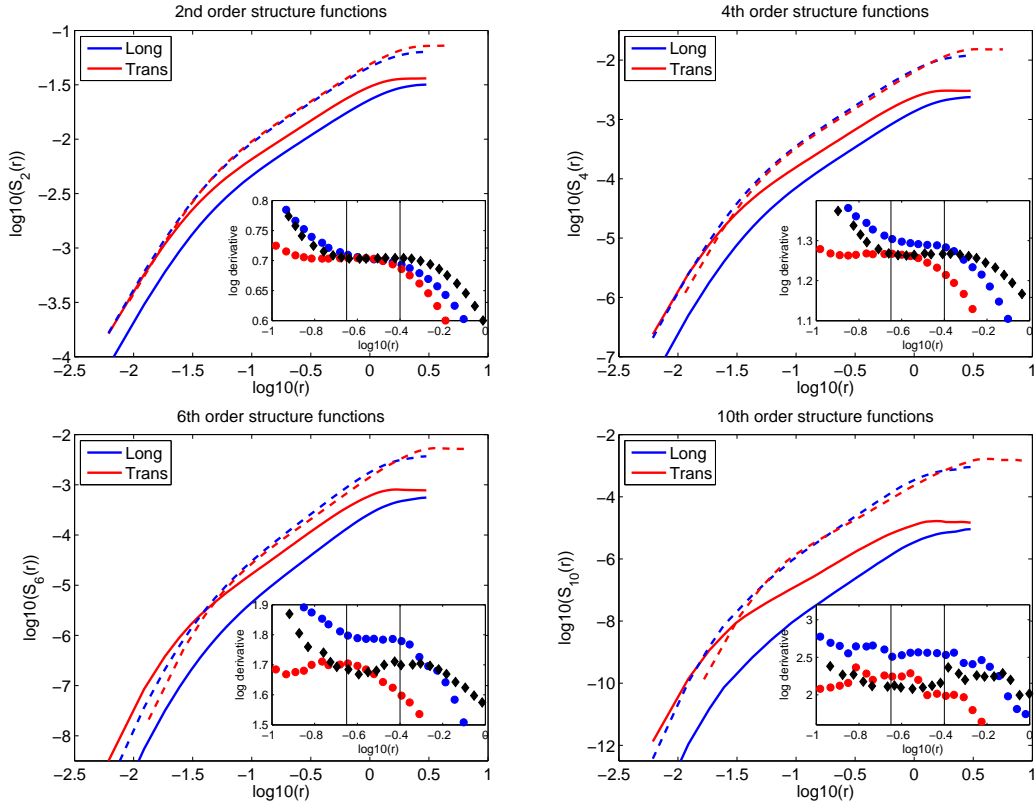


Figure 2. Structure functions of different order ($\mathcal{R}_\lambda = 460$). dashed lines: rescaled abscissa according to (6); solid lines: original (shifted vertically for clarity), Inset: logarithmic derivatives. black diamonds: rescaled transverse structure functions. vertical lines indicate the flat region of the third order structure function.

In addition, the range of scales over which a power-law behavior is observed is now identical for the two SFs, although the scaling exponents differ slightly. This is evidence in the inset of each sub-figure in Fig. 2 where the logarithmic derivatives of the structure functions with respect to scale have been plotted, and the vertical lines mark the scaling interval. Note, that both effects could not be achieved by an order-independent fixed rescaling factor of $3/2$.

For this data set the transverse increments are more intermittent than the rescaled ones. In order to address the question whether this difference in scaling might depend on Reynolds number, we show in Fig. 3 the logarithmic derivative of the 8th order structure function for three different simulations. With increasing Reynolds number the inertial range increases but the scaling exponent (value of the plateau) remains the same. We measure a value of approx. 2 for the transverse functions and 2.21 for the longitudinal ones. For comparison we included data from randomized snapshots originating from the simulation with $\mathcal{R}_\lambda = 730$. In detail, for each Fourier mode we change randomly the phase while preserving its amplitude and incompressibility of the flow. This preserves the energy spectrum but destroys the structure of the flow (energy cascade, coherent structures ...). The randomized longitudinal and transverse structure functions exhibit

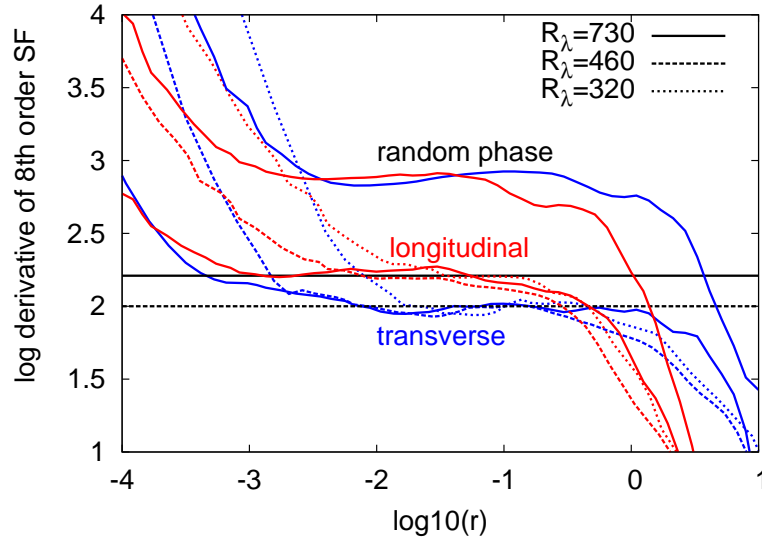


Figure 3. Logarithmic derivative of longitudinal and transverse structure functions for three different Reynolds numbers and in the case of a randomized velocity field.

the same scaling exponent, now close to the trivial $8/3$ value.

A general assumption is that possible remaining large scale anisotropy in the small scales is expected to decrease with Reynolds number. We remark that Biferale, Lanotte and Toschi [14] showed that the differences in the high-order exponents remain even if measured in the purely isotropic sector. That the curves in Fig. 3 fall on top of each other within the inertial range of scales is an indication that the observed differences in the scaling exponents are not due to large scale anisotropies. This indicates that the former observed differences have to be attributed to the specific small scale structures of the flow.

3. Implications for longitudinal and transverse PDFs

Since the rescaling property has the effect to make the longitudinal and transverse structure functions fall nearly on top of each other, we want to understand the effect of the rescaling transformation on the probability density functions (PDFs). In this subsection we try to map longitudinal PDFs to transverse ones using the rescaling property expressed through eqn. (8). The rescaling transformations were derived for even order structure functions. Thus in the following, we disregard skewness effects and consider only the symmetric part of the PDFs. We first approximate the numerically obtained longitudinal PDFs with a log-normal distribution using the expression given

Longitudinal and Transverse structure functions in high Reynolds-number turbulence 8
in Yakhot [22]

$$P_L(\Delta u, r) = \frac{1}{\pi \Delta u \sqrt{\ln r^b}} \int_{-\infty}^{\infty} e^{-x^2} \exp \left[-\frac{\left(\ln \frac{\Delta u}{r^a \sqrt{2x}} \right)^2}{4b \ln r} \right] dx \quad (10)$$

for which a fit is obtained with the values $a = 0.383$ and $b = 0.0166$ [22]. In Fig. 4 the numerically obtained PDF and the fit $P_L(\Delta u, r)$ are shown for several spatial scales. We apply the inverse Mellin transform

$$P_L(\Delta u, r) = \frac{1}{\Delta u} \int_{-i\infty}^{i\infty} dn S(n, r) (\Delta u)^{-n}$$

with $S(n, r) = A(n)r^{\xi(n)}$, and we follow the procedure in [22] which fixes the amplitude by going to the Gaussian limit for large spatial differences:

$$A(n) = (n-1)!! = \frac{2^{n/2}}{\sqrt{\pi}} \int_{-\infty}^{\infty} e^{-x^2} x^n dx$$

Now a mapping from the longitudinal PDFs to the transverse PDFs is obtained by inserting the rescaling relation (8) in the expression for the structure functions:

$$P_T(\Delta u, r) = \frac{1}{\Delta u} \int_{-i\infty}^{i\infty} dn A(n) (C(n)r)^{\xi(n)} (\Delta u)^{-n} \quad (11)$$

where $C(n) = \frac{\Gamma(n+2)}{2^n \Gamma^2(n/2+1)}$ as in eqn. (8).

Since the ansatz $S(n, r) = A(n)r^{\xi(n)}$ does not contain a cutoff at integral and at dissipation scales, this cutoff is inserted in the rescaling function $C(n)$. In both regions outside the inertial range smooth behavior is expected. On scales close to the integral range, Gaussian behavior for both longitudinal and transverse increments is expected and thus no rescaling is necessary. This justifies to choose $C(n)$ to be constant for $n \leq 0$. The cutoff at the dissipation scale is achieved by choosing $C(n)$ to be constant for $n > 6$. The precise value of the chosen n is dependent on the actual Reynolds number and the effect of choosing a different bound allows for a widening of the transformed PDF. This reflects the fact the Reynolds number has a similar effect on the width of the PDF. Evaluating the integral (11) using a saddle point approximation, we obtain a mapping from the log-normal fit of the longitudinal PDF $P_L(\Delta u, r)$ to a new PDF $P_T(\Delta u, r)$ which is compared to the numerically obtained data in Fig. 4 for increments ranging from the near dissipation range to integrals scales. One may observe that the agreement is especially remarkable in the inertial range ($r = 106\eta$ and $r = 212\eta$.) We do not expect perfect agreement for all scales since in that case there would be no room for differences between longitudinal and transverse structure functions. Thus the discrepancy for $r = 21\eta$ and $r = 42\eta$ just represents the missing contributions of the pressure term. Therefore, this method of mapping the PDFs is also a promising candidate for applications like PDF modeling of turbulent flows (see Pope [23] and references therein).

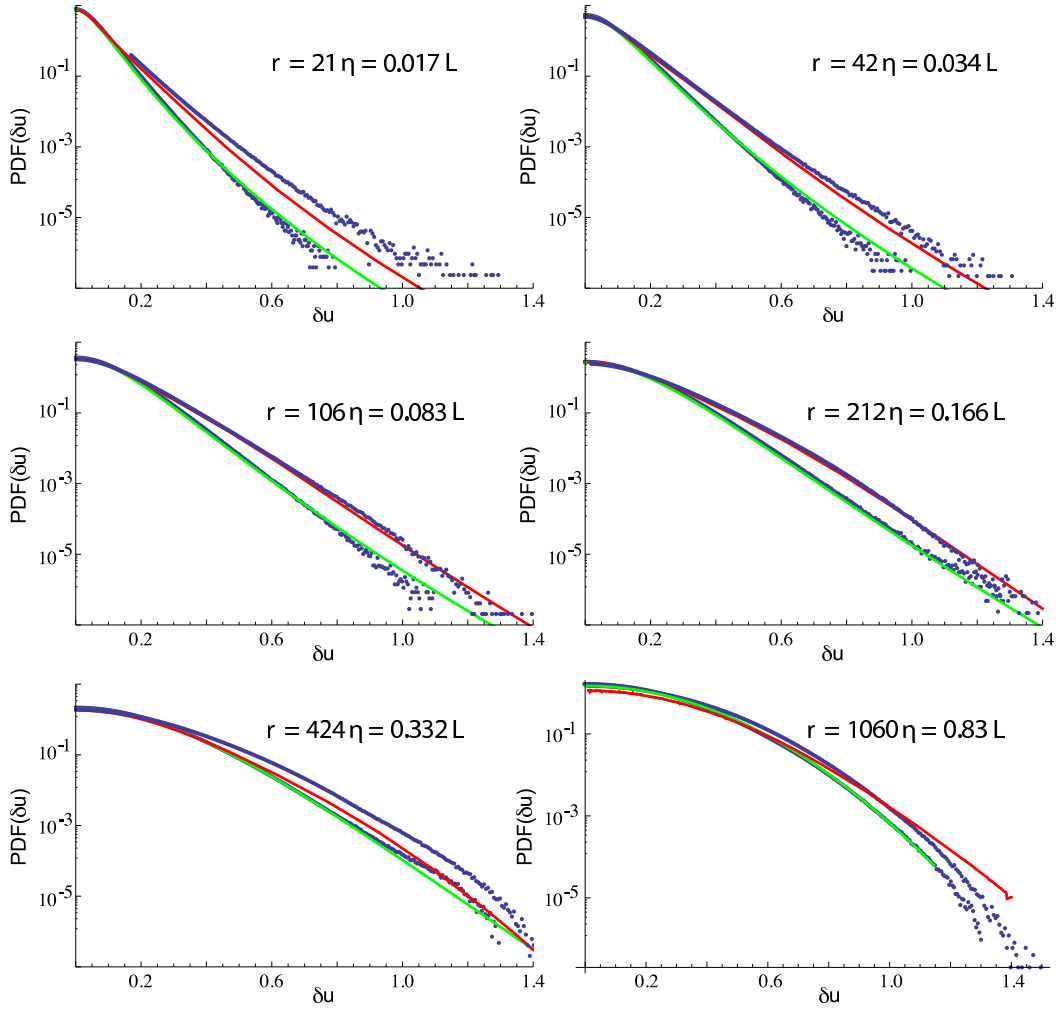


Figure 4. Longitudinal PDF (lower points) and fit with log-normal distribution (green line); transverse PDF (upper points) and mapped distribution (red line). Shown are the PDFs for different increments ranging from the near dissipation range to integrals scales. ($\Re_\lambda = 460$, η denotes the dissipation and L the integral scale.)

4. Conclusions and outlook

In this paper, we have suggested a new way of analyzing experimental and numerical data for longitudinal and transverse structure functions in Eulerian data of a turbulent velocity field. This procedure yields a mapping between the longitudinal and transverse scales, which provides consistent reference point in the identification of the inertial ranges of scales of turbulent flows. In addition, the derived scale correspondence allows for a direct mapping of the *full* probability density of transverse and longitudinal structure functions. This may be of much practical interest as the distributions carry a more complete information than a subset of their moments. The gap of longitudinal and transverse structure function exponents seems not to depend on Reynolds number but on small scale structure of the flow. The proposed mapping may help clarify the

role played by the pressure terms. Future work will be devoted to the analysis of other turbulent systems like magnetohydrodynamics, where the addition of the magnetic pressure term poses an interesting comparison.

Acknowledgments Access to the IBM BlueGene/P computer JUGENE at the FZ Jülich was made available through the 'XXL-project' of HBO28. This work benefited from partial support through DFG-FOR1048 in Germany, and ANR-07-BLAN-0155 in France.

References

- [1] Hill R 2001 *J. Fluid Mech.* **434** 379
- [2] Hill R and Boratav O 2001 *Phys. Fluids* **13** 276
- [3] Yakhot V 2001 *Phys. Rev. E* **63** 026307
- [4] Frisch U 1995 *Turbulence* (Cambridge: Cambridge University Press)
- [5] Biferale L and Procaccia I 2005 *Phys. Rep.* **414** 43
- [6] Noullez A, Wallace G, Lempert W, Miles R B and Frisch U 1997 *JFM* **339** 287–307
- [7] van de Water W and Herweijer J A 1999 *J. Fluid Mech.* **387** 3
- [8] Zhou T and Antonia R A 2000 *J. Fluid Mech.* **406** 81
- [9] Shen X and Warhaft Z 2002 *Phys. Fluids* **14** 370
- [10] Boratav O and Pelz R 1997 *Phys. Fluids* **9** 1400
- [11] Gotoh T, Fukayama D and Nakano T 2002 *Phys. Fluids* **14** 1065
- [12] Ishihara T, Gotoh T and Kaneda Y 2009 *Annu. Rev. Fluid Mech.*
- [13] Benzi R, Biferale L, Fischer R, Lamb D and Toschi F 2010 *J. Fluid Mech.* **653** 221–244
- [14] Biferale L, Lanotte A S and Toschi F 2008 *Physica D* **237** 1969 – 1975
- [15] Romano G P and Antonia R A 2001 *JFM* **436** 231–248
- [16] Germaschewski K and Grauer R 1999 *Phys. Plasmas* **6** 3788
- [17] Gotoh T and Nakano T 2003 *J. Stat. Phys.* **113** 855
- [18] Siefert M and Peinke J 2004 *Phys. Rev. E* **70** 015302
- [19] van Kármán T and Howarth L 1938 *Proc. R. Soc. London, Ser. A*
- [20] Kurien S and Sreenivasan K (2001) *Phys. Rev. E* **64** 056302
- [21] Homann H, Kamps O, Friedrich R and Grauer R 2009 *New Journal of Physics* **11** 73020
- [22] Yakhot V 2006 *Physica D* **215** 166–174
- [23] Pope S 2000 *Turbulent Flows* (Cambridge: Cambridge University Press)